

Molecular and functional analysis of Shiga toxin–induced response patterns in human vascular endothelial cells

Andreas Matussek, Joerg Lauber, Anna Bergau, Wiebke Hansen, Manfred Rohde, Kurt E. J. Dittmar, Matthias Gunzer, Michael Mengel, Patricia Gatzlaff, Maike Hartmann, Jan Buer, and Florian Gunzer

Enterohemorrhagic *Escherichia coli* (EHEC) is the major cause of hemolytic-uremic syndrome (HUS) characterized by microangiopathic hemolytic anemia, thrombocytopenia, and acute renal failure. EHEC produces one or more Shiga toxins (Stx1 and Stx2), and it was assumed that Stx's only relevant biologic activity was cell destruction through inhibition of protein synthesis. However, recent data indicate that in vivo the cytokine milieu may determine whether

endothelial cells survive or undergo apoptosis/necrosis when exposed to Stxs. In this study, we analyzed the genome-wide expression patterns of human endothelial cells stimulated with subinhibitory concentrations of Stxs in order to characterize the genomic expression program involved in the vascular pathology of HUS. We found that Stxs elicited few, but reproducible, changes in gene expression. The majority of genes reported in this study encodes for chemokines and

cytokines, which might contribute to the multifaceted inflammatory response of host endothelial cells observed in patients suffering from EHEC disease. In addition, our data provide for the first time molecular insights into the epidemiologically well-established higher pathogenicity of Stx2 over Stx1. (Blood. 2003;102:1323-1332)

© 2003 by The American Society of Hematology

Introduction

Enterohemorrhagic *Escherichia coli* (EHEC) is a major cause of serious outbreaks and sporadic cases of hemorrhagic colitis (HC) and hemolytic-uremic syndrome (HUS).^{1,2} Shiga toxin 2 (Stx2)–producing EHEC strains are more frequently associated with severe complications, such as HC and HUS.^{3–6} HUS is a systemic disease characterized by thrombotic microangiopathy (TMA) in affected organs,^{3,7} including kidneys, brain, and gastrointestinal tract. Because EHEC is a noninvasive pathogen, it is proposed that Stxs gain access to the systemic vasculature from the gut lumen and cause damage to endothelial cells in target organs,⁸ such as kidneys and central nervous system. Our understanding of these extraintestinal manifestations is still limited, and, for many years, it was assumed that the only relevant biologic activity of Stx was destruction of cells through inhibition of protein synthesis.⁹ Recently, however, several authors have described that treatment of various cell types with Stxs leads to increased mRNA levels as well as protein expression of chemokines¹⁰ and cell adhesion molecules.¹¹ C-X-C chemokines are involved in the chemoattraction and activation of neutrophils, while cell adhesion molecules mediate binding of inflammatory cells to the endothelium.¹² These findings indicate the important role of Stxs in inducing a multifaceted host inflammatory response. The inflammatory response of host endothelial cells seems to be a crucial step for developing the vascular damage observed in EHEC infection,³ ultimately resulting in TMA and HUS. Even subinhibitory

concentrations of toxins, exerting minimal influence on protein synthesis, were able to increase select mRNA transcript levels in endothelial cells very effectively, shown by Bitzan et al.¹³ These observations prompted us to investigate the regulatory effects of such concentrations of both Stx1 and Stx2 on human endothelial cells, using gene expression analysis arrays.

Furthermore, our interest was focused on identifying potential differences between the mode of action of Stx1 and Stx2 that could explain the high incidence of Stx2 producing *E coli* in patients with severe disease. Array data of selected genes were confirmed with real-time reverse-transcriptase polymerase chain reaction (RT-PCR). Whenever possible, expression of the corresponding proteins was assessed using enzyme-linked immunosorbent assay (ELISA), cytometric bead array (CBA),¹⁴ or fluorescence-activated cell sorter (FACS) analysis.

The present study surprisingly shows that only a limited subset of genes is regulated. Most of them belong to chemokines and cytokines. Other genes encode for cell adhesion molecules and transcription factors that are involved in immune response or apoptosis. These data indicate that subinhibitory concentrations of Stxs play an important role in inducing inflammatory responses of host endothelial cells. Such response patterns might well contribute to EHEC pathogenesis beyond the cytotoxic effects of Stxs caused by inhibition of protein biosynthesis in affected cells. The data presented also provide an explanation for the augmented pathogenicity of Stx2 over Stx1.

From the Mucosal Immunity Group, the Department of Microbiology, and the Department of Molecular Biotechnology, German Research Centre for Biotechnology (GBF), Braunschweig, Germany; the Institute of Medical Microbiology, Hannover Medical School, Hannover, Germany; the Department of Dermatology, University of Muenster, Muenster, Germany; and the Institute of Pathology, Hannover Medical School, Hannover, Germany.

Supported by the Deutsche Forschungsgemeinschaft, SFB 621.

Reprints: Florian Gunzer, Institute of Medical Microbiology, Hannover Medical School, Carl-Neuberg Strasse 1, D-30625 Hannover, Germany; e-mail: fgunzer@mikbio.h.shuttle.de.

The publication costs of this article were defrayed in part by page charge payment. Therefore, and solely to indicate this fact, this article is hereby marked "advertisement" in accordance with 18 U.S.C. section 1734.

© 2003 by The American Society of Hematology

Submitted October 30, 2002; accepted April 5, 2003. Prepublished online as *Blood* First Edition Paper, April 17, 2003; DOI 10.1182/blood-2002-10-3301.

Materials and methods

Stx purification

Stxs were purified on affinity columns according to a protocol described by Donohue-Rolfe et al¹⁵ with minor modifications. Liquid cultures of Stx2 producing EHEC strain 86-24¹⁶ and Stx1 expressing isolate EDL 973¹⁷ were grown in 5 liters of Luria-Bertani medium. After 4 hours of incubation, 0.4 mg/L mitomycin C (Sigma-Aldrich, Taufkirchen, Germany) was added to enhance Stx release from the bacteria, followed by 20 hours of incubation. Each culture was then centrifuged for 15 minutes at 16 000g (4°C), and the supernatant was retained and sterile filtered. A 70% ammonium sulfate precipitate of the supernatant was made and spun down for 10 minutes at 16 000g (4°C). The precipitate was dissolved in water and dialyzed against 10 mM Tris (tris(hydroxymethyl)aminomethane, pH 7.4) for 48 hours. The protein solution was then applied to an affinity column where a glycoprotein (B1011; Glycorex AB, Lund, Sweden; 200 µg/mL), containing a terminal galabiose bound to bovine serum albumin (BSA), acted as toxin receptor analog and was coupled to cyanogen bromide-activated Sepharose 4B (Pharmacia, Uppsala, Sweden) according to the manufacturer's protocol. The column was washed with 30 mL buffer (10 mM phosphate-buffered saline [PBS] pH 7.4, 1 M NaCl). For elution of toxin, a 4.5 M MgCl₂ solution was applied to the column with a gradient mixer. Pure Stx eluates showing 2 distinct bands on silver-stained sodium dodecyl sulfate (SDS) gels were pooled. To concentrate the toxin and remove MgCl₂, pooled samples were centrifuged over a Microcon YM-30 Centrifugal Filter Device (Millipore, Schwalbach, Germany) and washed repeatedly with 50 mL double distilled (dd) H₂O. A mock toxin preparation for incubation of control cells was made the same way, using liquid cultures of *E coli* TUV86-2, an isogenic Stx2-negative knock-out mutant of EHEC 86-24.¹⁸

SDS polyacrylamide gel electrophoresis and Western blot analysis

Stxs were separated on 15% SDS polyacrylamide gels (SDS-PAGE) using the Laemmli¹⁹ buffer system. For subsequent analysis of protein preparations, gels were stained with silver nitrate^{20,21} (Figure 1A). Proteins were then electrotransferred onto nitrocellulose membranes using a semidry blotting system from Biometra (Goettingen, Germany) and probed with either rabbit or pig polyclonal sera (diluted 1:2000) against Stx1 or Stx2. Bound primary antibodies were detected with alkaline phosphatase-labeled secondary antibodies and visualized with bromo chloro indolyl phosphate/nitroblue tetrazolium (BCIP/NBT; Roche Diagnostics, Mannheim, Germany) as substrate/color reagent (Figure 1B).

LPS quantification

Quantification of lipopolysaccharide (LPS) in Stx preparations and the mock toxin was carried out using Endosafe Limulus Amebocyte Lysate (LAL) test, which gives the opportunity to quantify the amount of endotoxin photometrically, from Charles River Laboratories (Sulzfeld, Germany). End-point method, following the protocol supplied by the manufacturer, was used to determine LPS concentration in each toxin preparation used in subsequent experiments.

Human umbilical vein endothelial cells (HUVECs)

Human endothelial cells were provided by CellSystems (St Katharinen, Germany) and cultured in Endothelial Cell Growth Medium BulletKit-2 (CellSystems), containing all required supplements. Cells were maintained in 95% air/5% CO₂ at 37°C. Stxs were added to confluent monolayers of HUVECs at 1/10 median lethal dose (LD₅₀) diluted in dd H₂O. Negative controls were incubated with an identical volume of mock toxin, which had been analyzed by SDS-PAGE and tested for cytotoxic activity.

Cytotoxicity assay

Cytotoxic activity of Stx preparations and the mock toxin was measured with the Cytotoxicity Detection Kit from Roche Diagnostics, which is

based on detection of lactate dehydrogenase (LDH) activity released from damaged cells. When LDH is present in the culture supernatant, a color reaction is induced by cleavage of a tetrazolium salt. HUVECs were incubated with serial dilutions from 50 µg/mL to 10 pg/mL of the 2 protein toxins for 48 hours in a 96-well micro plate (Greiner Bio-One, Frickenhausen, Germany). After incubation, the plate was centrifuged and from each well 100 µL cell-free culture supernatant was transferred to another micro plate. Substrate mixture was then added and incubated at room temperature for 30 minutes. Absorbance was measured at 492 nm using an ELISA plate reader (Titertek Multiscan Ascent; Dunn Labortechnik, Asbach, Germany). Triton X-100, which induces complete cell lysis, was used as positive control. Supernatants from untreated cells were used as low control. All tests were performed in triplicate and were repeated once.

Immunohistochemistry

Slides with HUVEC cytopins were fixed in ice-cold acetone at -20°C for 10 minutes and air dried. After blocking endogenous biotin by incubation with avidin and biotin (Vector Laboratories, Burlingame, CA), the slides were incubated with a monoclonal rat antihuman CD77 immunoglobulin M (IgM) antibody (Beckman Coulter, Unterschleissheim, Germany; clone 38-13, diluted 1:10), which specifically recognizes the terminal galabiose residue from the Stx receptor Gb3Cer. A biotinylated rabbit antirat IgM (Dianova, Hamburg, Germany; diluted 1:250) served as secondary antibody and was detected with an alkaline phosphatase-conjugated streptavidin complex (DAKO, Hamburg, Germany). Fast red (Sigma-Aldrich) served as substrate and hemalaun as counterstain. Cells were washed thoroughly with buffer (0.1 M Tris-HCl, 0.15 M NaCl, 0.05% Tween 20) after each incubation step. Appropriate negative controls without primary antibody were processed in parallel.

Transmission electron microscopy: preparation of Stx2 protein-coated colloidal gold particles

Adjusted with 25 mM K₂CO₃ to pH 6.2 was 5 mL of a colloidal gold-particle solution (20 nm in size; BioCell, Cardiff, United Kingdom). Then, 5 µL Stx2 protein (10 mg/mL stock solution) was added to 5 mL of the colloidal gold solution and incubated for 30 minutes at room temperature. Stx2 gold complexes were centrifuged at 20 000 rpm for 15 minutes in a Beckman TLD100 (Beckman Coulter). The resulting red pellet was gently resuspended in PBS buffer containing 2 mg/mL polyethyleneglycol (PEG 20 000; Mallinckrodt Baker, Griesheim, Germany) for stabilization of protein-gold complexes. Negative staining revealed more than 90% single Stx2 gold particles. For incubation of control cells, gold particles were coated with BSA (7 µg BSA/mL gold-particle solution).

Incubation of HUVECs with Stx2 gold particles and embedding

Subconfluent monolayers of HUVECs were grown in 6-cm petri dishes and incubated with Stx2 gold particles (1:20 dilution of the stock solution) or BSA gold particles (1:20 dilution of the stock solution). At different time points the endothelial cells were fixed with a fixation solution containing 2% glutaraldehyde and 3% formaldehyde in cacodylate buffer for one hour on ice. After several washing steps with cacodylate buffer, cells were further fixed and contrasted with 1% aqueous osmium tetroxide for 2 hours at room temperature, and subsequently washed with cacodylate buffer. Cells were scraped off the petri dish and pelleted. Embedding in Spurr resin was done according to described procedures.²²

RT-PCR

RNA was extracted using TriFast FL (peqLab, Erlangen, Germany) according to the manufacturer's protocol, and reversely transcribed with 200 U Moloney murine leukemia virus (M-MLV) reverse transcriptase (Gibco, Karlsruhe, Germany) for 45 minutes at 42°C in 20-µL assays containing 1 µL Oligo dT-primers (Gibco) and 10 mM deoxynucleoside triphosphates (dNTPs), following the manufacturer's instructions. The reaction was stopped by adding 40 µL Tris-ethylenediaminetetraacetic acid (EDTA) buffer (pH 8.0) and performing heat inactivation for 10 minutes at 90°C. Table 1 provides all genes with corresponding primers (synthesized

Table 1. Primers used for real-time RT-PCR

Product	5' Sequence 3'	Sense/antisense	Product length, bp	T _m , °C
CSF2	GGC CAG CCA CTA CAA GCA GCA CT	Sense	119	61.4
	CAA AGG GGA TGA CAA GCA GAA AG	Antisense		56.7
EGR-1	GAT CTC GGC TCA CTG CAA CCT CTG	Sense	167	61.5
	CCA AGC CAG CGG GAA TG	Antisense		58.5
GRO-1	CTC TAC CTG CAC ACT GTC CTA TTA	Sense	178	50.1
	ATC CGC CAG CCT CTA TCA	Antisense		50.3
GRO-2	TTT TAG GTC AAA CCC AAG TTA GTT	Sense	150	50.6
	TTC TTG GAT TCC TCA GCC TCT ATC	Antisense		54.6
GRO-3	AAG AAG CTT ATC AGC GTA TCA T	Sense	150	54.7
	AAT AAG TAG AAC CCT CGT AAG AAA	Antisense		55.9
ICAM1	TGC CCG AGC TCA AGT GTC TA	Sense	225	53.3
	GCC TGC AGT GCC CAT TAT	Antisense		50.7
IL-6	CAC CCC TGA CCC AAC CAC AAA T	Sense	105	59.3
	TCC TTA AAG CTG CGC AGA ATG AGA	Antisense		59.2
IL-8	GAC CAC ACT GCG CCA ACA CA	Sense	117	57.6
	CAG CCC TCT TCA AAA ACT TCT CCA	Antisense		57.8
LAMB3	CAG ACG CAC ACG GCT CCT AAT CCA	Sense	225	63.9
	CGG GCA CGC GCA ATG TCC T	Antisense		63.6
MCP-1	GTC TCT GCC GCC CTT CTG TG	Sense	94	63.5
	AGG TGA CTG GGG CAT TGA TTG	Antisense		59.8
NFκB2	TGC CAA ACA GAT TCC CAA AGT AGT	Sense	155	55.9
	CAA GGA GAT GCA AAT TCA AAC ACA	Antisense		55.8
RPS-9	CGC AGG CGC AGA CGG TGG AAG C	Sense	92	61.1
TRAF-1	CGA AGG GTC TCC GCG GGG TCA CAT	Antisense	144	60.5
	GGG GCA TAA ACT TTC CTC TTC C	Sense		60.3
	TTT GGG GTT ATA CAT TGC TCA GTG	Antisense		59.3

CSF2 indicates colony stimulating factor 2 (granulocyte-macrophage); EGR-1, early growth response 1; GRO-1, GRO-1 oncogene; GRO-2, GRO-2 oncogene; GRO-3, GRO-3 oncogene; ICAM1, intercellular adhesion molecule-1; IL-6, interleukin 6; IL-8, interleukin 8; LAMB3, laminin beta 3; MCP-1, monocyte chemotactic protein 1; NFκB2, nuclear factor of kappa light polypeptide gene enhancer in B-cells 2; RPS-9, ribosomal protein S9; TRAF-1, TNF receptor-associated factor 1; and T_m, melting temperature.

by MWG-Biotech, Ebersberg, Germany) used for conventional and real-time PCR. Conventional PCR was performed with 0.5 U BioThermStar KlenTaq polymerase (GENECRAFT, Muenster, Germany) in 20 μL-assays containing 0.25 pmol primers and 0.5 mM dNTP using the following cycling conditions: activation of Taq polymerase for 7 minutes at 95°C, followed by 35 cycles each consisting of a 10-second denaturing interval at 94°C, a 20-second annealing step at 54/58°C (depending on primer T_m), and a primer extension at 72°C for 20 seconds. Amplification was finished with a final extension at 72°C for 5 minutes. PCR products were resolved by electrophoresis on 2.0% agarose gels and visualized by ethidium-bromide staining.

Incubation of HUVECs with Stxs and labeling of RNA

HUVECs were grown to confluence in 75 cm² flasks. Cell culture medium was replaced prior to adding 1/10 LD₅₀ of Stx1 or Stx2 to 2 flasks each. Another 2 flasks were kept as control. Cells were incubated at 37°C for either 4 hours or 24 hours and immediately used for RNA isolation. Total RNA was extracted using TriFast FL (peqLab) as described by the manufacturer. RNA was converted to double-stranded cDNA using a modified oligo-dT primer with a 5' T7 RNA polymerase promoter sequence and the Superscript Choice System (Gibco) for cDNA synthesis. Double-stranded cDNA was purified by phenol-chloroform extraction and ethanol precipitation. Then, *in vitro* biotin-labeled cRNA transcription was performed using T7 RNA polymerase and the cDNA template in the presence of a mixture of unlabeled nucleotides (adenosine triphosphate [ATP], cytidine triphosphate [CTP], guanosine triphosphate [GTP], and uridine triphosphate [UTP]) and biotin-labeled CTP and UTP (BioArray High Yield RNA Transcript Labeling Kit; Enzo Diagnostics, Farmingdale NY). Biotin-labeled cRNA was then purified on microspin columns provided with the RNeasy Mini Kit from QIAGEN (Hilden, Germany) and fragmented according to the Affymetrix (Santa Clara, CA) protocol. The amount of labeled cRNA was determined by measuring absorbance at 260 nm.

Hybridization and scanning of gene expression analysis arrays

To monitor the relative abundance of mRNA for full-length human genes, the Affymetrix GeneChip HuGeneFL (6800 genes) system was used for Stx1 experiments and HG_U95v2 (12 488 genes) for Stx2 experiments. All regulated genes shown in Table 2 were present on both types of Affymetrix GeneChips. Labeled cRNA, fragmented to an average size of 100 to 150 bases, was hybridized to the GeneChips. The cRNA fragments were heated in a hybridization solution to 99°C for 5 minutes and then cooled at 45°C for 5 minutes before being injected into the Affymetrix reaction chamber. Hybridization was carried out at 45°C for 16 hours after which arrays were washed in an automated Affymetrix fluidic station. Hybridized cRNA was fluorescently labeled by adding streptavidin-phycoerythrin (Molecular Probes, Eugene, OR) as previously described by Lockhart et al.²³ Unbound streptavidin-phycoerythrin was removed by rinsing the probe arrays at room temperature. Stained arrays were scanned at 488-nm excitation wavelength in a Hewlett-Packard Gene Array Scanner (Agilent Technologies, Palo Alto, CA). A complete list of genes present on HuGeneFL and on HG_U95v2 can be found in the Affymetrix database at <http://www.affymetrix.com/analysis/index.affx>.

Data analysis

Data were analyzed using Affymetrix Microarray Suite 5.0. Using the Affymetrix Data Mining Tool (DMT), gene expression was evaluated and genes with at least a 2-fold or greater change in signal intensity in 2 independent experiments were considered regulated. In the DMT, *P* values were set to less than .001 for up-regulated genes and set to more than .999 for down-regulated ones (no down-regulated genes in our experiments).

Quantitative real-time RT-PCR

Quantitative real-time PCR was performed from 2 independent experiments with a GeneAmp 5700 Sequence Detection System (Applied Biosystems, Weiterstadt, Germany) to quantify mRNA levels of selected genes.

Table 2. Genes differentially expressed in HUVECs stimulated with Stxs

Functional category	Gene symbol	GB Acc. no.	Fold change				Putative function	
			Stx1		Stx2			
			4 h	24 h	4 h	24 h		
General metabolism	<i>EPB41</i>	M61733	—	4.7	—	—	Protein 4.1 is a major structural element of the erythrocyte membrane skeleton. It plays a key role in regulating physical properties of membranes such as mechanical stability and deformability by stabilizing spectrin-actin interactions. Binds with a high affinity to glycophorin and with lower affinity to bandprotein.	
	<i>GPX4</i>	AC005390	—	—	—	4.5	Could play a major role in protecting mammals from the toxicity of ingested lipid hydroperoxides.	
	<i>MMP9</i>	J05070	—	—	4.5	—	Could play a role in osteoclast resorption.	
Secreted	<i>CSF2</i>	M13207	—	3.6	6.9	8.2	Cytokine that stimulates growth and differentiation of hematopoietic precursor cells of different lineages.	
	<i>GRO-1</i>	X54489	21.3	8.7	10.6	16.1	Chemotactic activity for neutrophils. Plays a role in inflammation and exerts its effects on endothelial cells in an autocrine fashion.	
	<i>GRO-2</i>	M36820	—	23.8	55.0	14.5	Produced by activated monocytes and neutrophils and expressed at sites of inflammation.	
	<i>GRO-3</i>	M36821	—	4.6	—	4.3	Plays a role in inflammation and exerts its effects on endothelial cells in an autocrine fashion.	
	<i>IL-6</i>	X04430	—	—	—	2.7	Plays an essential role in the final differentiation of B cells into Ig-secreting cells, induces myeloma and plasmacytoma growth.	
	<i>IL-8</i>	M17017	4.3	17.4	14.9	26.6	Chemotactic factor that attracts neutrophils, basophils, and T cells also involved in activation of neutrophils.	
	<i>IL-16</i>	M90391	—	—	5.3	—	Stimulates a migratory response in CD4 lymphocytes, monocytes, and eosinophils.	
	<i>MCP-1</i>	M26683	—	—	15.9	6.6	Chemotactic factor that attracts monocytes and basophils.	
	Signaling	<i>DUSP1</i>	X68277	2.1	—	—	—	Dual specificity phosphatase that dephosphorylates map kinase ERK2 on both Thr183 and Tyr185.
		<i>GNA13</i>	L22075	—	4.6	—	—	Guanine nucleotide-binding proteins (g proteins) are involved as modulators or transducers of various transmembrane signaling systems.
<i>GOS2</i>		M69199	—	—	3.0	—	Potential oncogene and regulator of latent HIV.	
<i>NK4</i>		AA631972	—	—	—	3.1	May play a role in lymphocyte activation.	
<i>PPARA</i>		L02932	—	—	6.3	—	Controls the peroxisomal Beta-oxidation pathway of fatty acids.	
<i>PRP4</i>		U48736	—	2.2	—	—	A protein kinase that appears to be involved in pre-mRNA splicing.	
<i>PTGS2</i>		L15326	4.9	—	—	—	May have a role as a major mediator of inflammation and/or a role for prostanoid signaling in activity-dependent plasticity.	
<i>RYR1</i>		U48508	—	—	4.8	—	Communication between transverse tubules and sarcoplasmic reticulum. Contraction of skeletal muscle is triggered by release of calcium ions from SR following depolarization of T tubules.	
<i>ZFP36</i>		M92843	3.2	—	2.4	—	Regulatory protein with a novel zinc finger structure involved in regulating the response to growth factors. Has been shown to bind zinc.	
Surface receptors		<i>ALCAM</i>	U30999	2.7	—	—	—	Cell adhesion molecule that binds to CD6. Involved in neurite extension by neurons via heterophilic and homophilic interactions. May play a role in the binding of T and B cells to activated leukocytes, as well as in interactions between cells of the nervous system.
	<i>ICAM1</i>	M24283	—	4.6	12.7	20.7	Ligand for the leukocyte adhesion LFA-1 protein.	
	<i>KIR2DL3</i>	AC006293	—	—	8.1	—	Receptor on natural killer cells for HLA-C alleles. Inhibits the activity of NK cells thus preventing cell lysis.	
	<i>LAMB3</i>	U17760	—	4.9	—	3.4	Binds to cells via a high-affinity receptor. Laminin is thought to mediate attachment, migration, and organization of cells into tissues.	
Transcription and translation factors	<i>ATF3</i>	L19871	—	3.8	2.0	—	Represses transcription from promoters with ATF sites.	
	<i>CEBPD</i>	M83667	—	—	—	2.8	Important transcriptional activator in the regulation of genes involved in immune and inflammatory responses.	
	<i>EGR-1</i>	X52541	3.8	2.3	—	—	Transcriptional regulator. Recognizes and binds to the DNA sequence 5'-cgccccgc-3' (egr-1 site). Activates the transcription of target genes whose products are required for mitogenesis and differentiation.	
	<i>FOS</i>	V01512	10.8	—	—	—	Nuclear phosphoprotein that forms a tight but noncovalently linked complex with the c-jun/AP-1 transcription factor. c-fos has a critical function in regulating the development of cells destined to form and maintain the cytoskeleton. It is thought to have an important role in signal transduction, cell proliferation, and differentiation.	
	<i>FOSL2</i>	X16706	—	6.5	—	—	Fos-related antigen 2.	
	<i>GEM</i>	U10550	—	3.8	—	—	Possible regulatory protein, possibly participating in receptor-mediated signal transduction at the plasma membrane. Has guanine nucleotide-binding activity but undetectable intrinsic GTPase activity.	
	<i>JUNB</i>	U20734	2.8	2.4	—	—	Transcription factor involved in regulating gene activity following the primary growth factor response. Binds to the DNA sequence tgac/gtca.	
	<i>NFκB2</i>	S76638	—	—	—	2.5	p100 is the precursor of the p52 subunit of the NF-Kappa-B, which binds to the Kappa-B consensus sequence, located in the enhancer regions of genes involved in immune response and acute-phase reactions.	
	<i>NFκBIA</i>	M69043	—	—	2.6	—	Involved in regulation of transcriptional response of NF-Kappa-B, including adhesion-dependent pathways of monocyte activation.	

Table 2. Genes differentially expressed in HUVECs stimulated with Stxs (continued)

Functional category	Gene symbol	GB Acc. no.	Fold change				Putative function
			Stx1		Stx2		
			4 h	24 h	4 h	24 h	
	<i>SNAPC1</i>	U44754	—	6.7	—	—	Complex required for the transcription of both RNA polymerase and small nuclear RNA genes. Binds to the proximal sequence element (PSE), a non-tata-box basal promoter element common to these 2 types of genes.
	<i>TNFαIP-3</i>	M59465	—	3.7	—	11.2	Inhibitor of programmed cell death. May contribute to the in vivo effects of TNF.
	<i>TRAF-1</i>	U19261	—	4.3	—	32.9	Signal transducer associated with the cytoplasmic domain of the tumor necrosis factor receptor (TNF-R2).
Unknown		U17760	—	2.7	—	—	∅
		U38372	—	3.2	—	—	∅

Fold change is the factor of regulation of mRNA from Stx-stimulated HUVECs versus nonstimulated HUVECs. Genes were included in this table if they were up- or down-regulated in 2 independent experiments by a factor of 2 or higher. Data are presented as mean value of regulation ($n = 2$). GB Acc no. indicates GenBank accession number; —, no regulation; NK, natural killer; SR, sarcoplasmic reticulum; LFA-1, leukocyte function-associated molecule 1; ATF, activating transcription factor; and ∅, putative function not known.

Amplifications were run in 50- μ L assays with the TaqMan Universal Master Mix (Applied Biosystems) containing SYBR-Green and PCR core reagents, according to the manufacturer's protocol. The cycling program was as follows: initial annealing for 2 minutes at 50°C followed by activation of Taq polymerase for 10 minutes at 95°C. Then, 40 amplification cycles of a 15-second denaturing interval at 95°C and a one-minute annealing step at 54/58°C (depending on primer T_m) were run. Standard curves were generated using serially diluted cDNA probes. The RPS9 housekeeping gene²⁴ was used for normalization.

Flow cytometry

Monoclonal antibodies (mAbs) directed against the following molecules were used for staining: CD31 (platelet endothelial cell adhesion molecule, PECAM-1), CD34, CD54 (intercellular adhesion molecule-1), CD62E (E-selectin), CD62P (P-selectin), CD106 (vascular cell adhesion molecule-1, VCAM-1), CLA (cutaneous lymphocyte-associated antigen), and isotype. Antibodies were purchased from BD PharMingen (Heidelberg, Germany) and Immunotech (Unterschleissheim, Germany). Stimulated and unstimulated HUVECs were removed from flasks using Accutase (Innovative Cell Technologies, San Diego, CA) and stained in NUNC round-bottom 96-well plates (Fisher Scientific, Nidderau, Germany) (2×10^5 cells/well) in 20 μ L of mAb in PBS/2% fetal calf serum (FCS) for 20 minutes on ice. Single-color immunocytometry was performed with a FACSCalibur flow cytometry system (BD Biosciences, Heidelberg, Germany). Each antibody was tested in 3 independent experiments. Acquired data were analyzed using the WinMDI 2.8 software package (www.facs.scripps.edu/software.html; Scripps Institute, La Jolla, CA).

Cytometric bead array (CBA)

The CBA consists of a series of spectrally discrete particles that can be used to detect soluble analytes by flow cytometry. Microparticles with covalently bound antibodies, as previously described by Chen et al,¹⁴ were purchased from Becton Dickinson (Heidelberg, Germany). Briefly, polystyrene beads (7.5- μ m diameter) are dyed to 6 different fluorescence intensities, which have an emission wavelength of approximately 650 nm (FL-3). Each group carries antibodies against one of the 6 following cytokines: IL-1 β (interleukin 1 β), IL-6 (interleukin 6), IL-8 (interleukin 8), IL-10 (interleukin 10), IL-12p70 (interleukin 12p70), TNF- α (tumor necrosis factor α), representing a unique population in FL-3 intensity. The Ab-labeled particles serve as capture for a given cytokine in the immunoassay panel and can be identified simultaneously in a mixture. The captured cytokines are then detected using 6 specific antibodies coupled to phycoerythrin (PE), which emits its fluorescence at approximately 585 nm (FL-2). Predefined mixtures of all 6 cytokines served as calibrators (standards ranging from 0 to 5000 pg/mL) for the assay system. Added to a mixture of each 50- μ L capture Ab-bead reagent and detector Ab-PE reagent was 50 μ L of sample or cytokine standard. The mixture (150 μ L) was incubated for 3 hours at room temperature and washed to remove unbound detector Ab-PE reagent before data acquisition using flow cytometry. Using a FACSCalibur flow cytom-

eter, 2-color flow cytometric analysis was performed. Acquired data obtained from 3 independent experiments were analyzed using Becton Dickinson Cytometric Bead Array software.

GM-CSF, GRO-1, and MCP-1 ELISA

Granulocyte-macrophage colony-stimulating factor (GM-CSF), GRO-1, and MCP-1 proteins in supernatants of control cells and cells treated with Stxs were quantified by enzyme immunoassay using standards ranging from 7.8 to 500 pg/mL (GM-CSF) and from 15.6 to 1000 pg/mL (GRO α and MCP-1) according to the manufacturer's protocol (Quantikine Human GM-CSF and Human GRO α Immunoassay from R&D Systems, Wiesbaden, Germany; and Human MCP-1 OptEIA Kit from BD Biosciences). Tissue culture supernatants from 3 independent experiments were used for ELISA testing.

Results

Isolation of Stxs and cytotoxicity testing

Using receptor affinity chromatography, we managed to isolate highly pure Stx preparations, with no contaminations as documented by SDS-PAGE and Western blotting. In Figure 1A, purified Stx2 is exemplified, separated on an SDS gel, and visualized with silver stain. The A-subunit has a molecular mass of 32 kDa and monomeric B-subunits are resolved at 7.7 kDa. Identity of Stx2 protein was confirmed with Western blot analysis, as shown in Figure 1B. Purity of Stx1 preparations was comparable. All toxin preparations contained only very low amounts of lipopolysaccharide ranging from 2.0 to 2.4 EU/mL, which equals 0.20 to 0.24 ng LPS/mL of concentrated protein

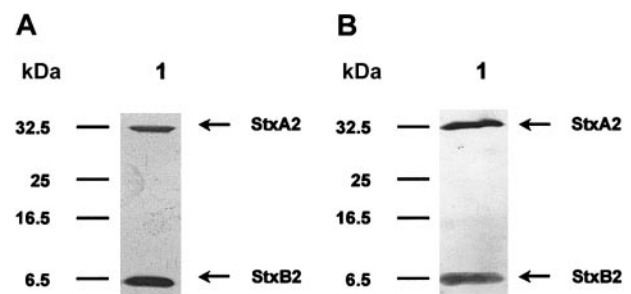


Figure 1. SDS-PAGE and Western blotting of purified Stx2. Stx2 holotoxin was purified by affinity chromatography using a receptor analog. In panel A, a silver-stained SDS gel is shown. The cytotoxic A-subunit has a molecular mass of 32 kDa and monomeric B-subunits are separated at 7 kDa. Panel B pictures a Western blot analysis of this toxin molecule, using polyclonal rabbit anti-Stx2 antibodies. The protein preparation is free of any visible contamination.

solution. LPS concentration in the mock toxin preparation, used for incubation of control cells, was comparable. Therefore, an influence of bacterial lipopolysaccharide on the regulatory phenomena observed in the following cell culture assays was excluded. Evaluation of cytotoxic activity of the 2 different Stxs resulted in LD₅₀ values of approximately 3 μg/mL for Stx1 and approximately 4 μg/mL for Stx2. The mock toxin was neither cytotoxic nor did it contain any stainable protein.

Distribution of Stx receptors on HUVECs and cellular uptake of Stxs

Immunohistochemistry of HUVECs showed a dense seam of Stx receptors at the cell surface, demonstrated by the intense red linear membrane stain shown in Figure 2. Incorporation of gold-labeled Stx was observed in endothelial cells as early as 15 minutes after administration. Differences in toxin uptake between Stx1 and Stx2 could not be determined, with regard to amount of toxin and time kinetic. No uptake of BSA gold particles was observed with the control cells (not shown). In Figure 3, HUVECs are shown after incubation with Stx2 for 1 hour (Figure 3A) and 4 hours (Figure 3B). After 4 hours the toxin has almost entirely been endocytosed by the cells.

Array analysis

Gene expression analysis performed on HUVECs after incubation with 1/10 LD₅₀ Stx1 or Stx2 for 4 hours and 24 hours revealed that only a small number of genes was regulated, despite the fact that the microarrays we had used represented 6800 (Stx1 experiments: 9 genes regulated after 4 hours and 20 genes regulated after 24 hours) and 12 488 (Stx2 experiments: 15 genes regulated after 4 hours and 24 hours) human genes. Most of them belonged to chemokines and cytokines. Other genes encoded for cell adhesion molecules and transcription factors that are involved in immune response or apoptosis. Table 2 shows the ratio of gene expression in HUVECs treated with each toxin compared with untreated control cultures. In our experiments, only up-regulation of genes was observed. The highest increase in mRNA levels was found for IL-8, GRO-1, and GRO-2 after treatment with either one of the 2 toxins. A group of genes was exclusively regulated by incubation with Stx2, among these the coding sequences for IL-6, IL-16, MCP-1, and NFκB2. This toxin molecule also had a marked effect on up-regulation of CSF2 and ICAM1 genes after 4 hours and 24

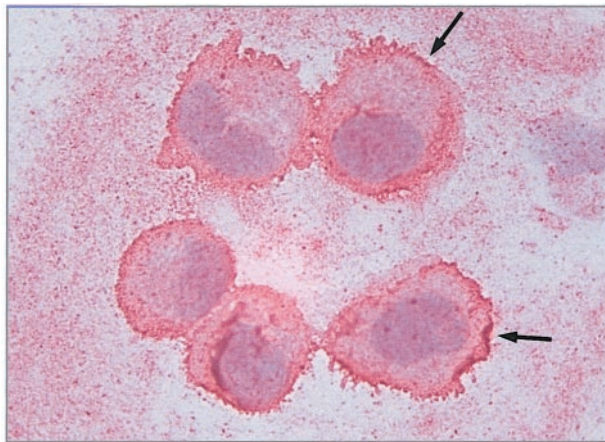


Figure 2. Immunostaining of Stx receptors. Immunohistochemical detection of the Stx receptor Gb3/CD77 on 5 single endothelial cells (HUVEC) immobilized onto glass slides by cytoentrifugation was performed with avidin biotin complex technique using a monoclonal rat antihuman CD77 primary antibody. Binding of the antibody is pictured as a red linear membrane stain (arrows, × 630).

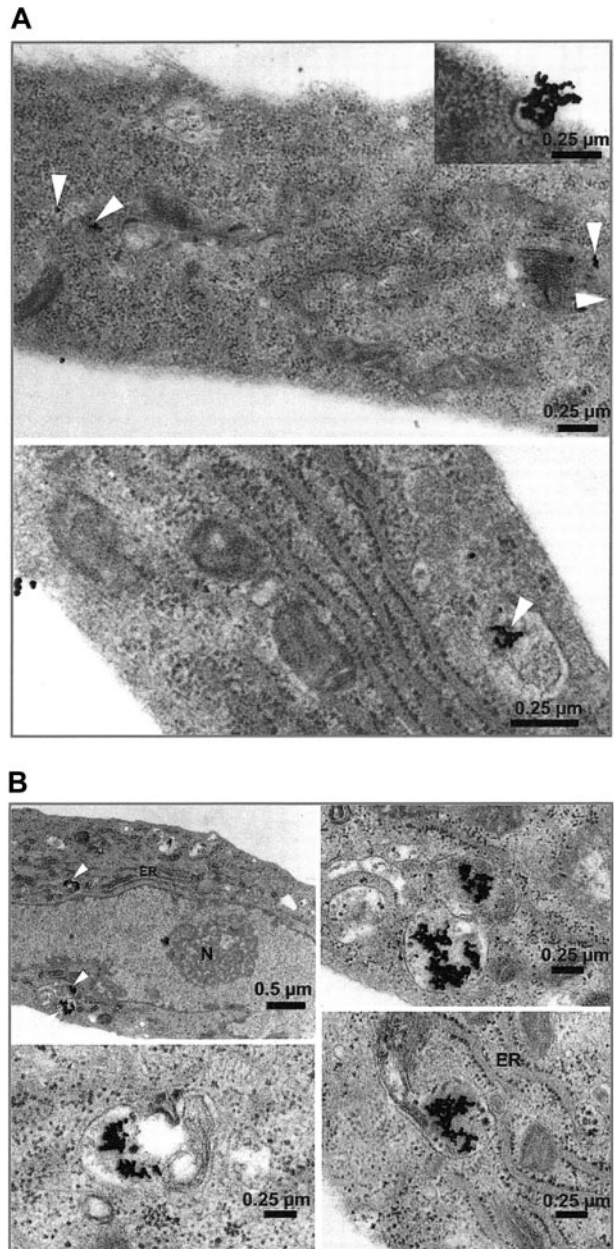


Figure 3. Uptake of gold-labeled Stx2. HUVECs treated with gold-labeled Stx2 were fixed after 1 hour (A) and 4 hours (B) and scanned with a transmission electron microscope. Black beads, marked intracellularly with white arrowheads, correspond to gold-labeled Stx2. Uptake of Stx2 and intracellular distribution after one hour is visualized in panel A. At 4 hours most of the toxin is detected intracellularly as shown in panel B. ER indicates endoplasmic reticulum; N, nucleus.

hours, while Stx1 led to only a moderately increased gene expression after 24 hours. In contrast, EGR-1, FOS, and JUNB mRNA were expressed only after Stx1 treatment. Regulation of genes encoding GRO-3, LAMB3, tumor necrosis factor, α-induced protein 3 (TNFαIP-3) and TRAF-1 was first observed after incubation for 24 hours with both toxins, as opposed to zinc finger protein 36 (ZFP36), which was induced at 4 hours but did not reveal any gene expression after 24 hours.

Quantitative real-time RT-PCR

Regulatory effects observed by array analysis were further studied by real-time RT-PCR for 12 selected genes. For these experiments, HUVECs were treated with Stxs the same way as they were for

array analyses. Real-time RT-PCR data are presented in Figure 4. As a rule, array data could be confirmed by quantitative real-time RT-PCR for *CSF2*, *EGR-1*, *ICAM1*, *IL-6*, *IL-8*, *LAMB3*, *NFκB2*, and *TRAF-1*. However, real-time RT-PCR analysis revealed that *MCP-1* was also regulated in cells treated with Stx1, which was in marked contrast to array data. Furthermore, the pattern of regulation between the different members of the GRO family differed from the data obtained by microarray analysis. MCP-1 and GRO-1 were therefore further studied at the protein level.

Flow cytometry and protein assays

Investigation of HUVECs treated with Stxs by flow cytometry showed expression of ICAM1 and CD62P on the cell surface exclusively after incubation with Stx2 for 24 hours (Figure 5A-B). FACS analysis with antibodies directed against CD31, CD34, CD62E, CD106, and CLA antigens showed no difference between control cells and HUVECs incubated with Stxs (data not shown). CBA analysis revealed increased levels of IL-6 and IL-8 after 24 hours in cell culture supernatants of HUVECs treated with Stx1 as well as with Stx2, as shown in Figure 6A-B. In contrast, IL-1β, IL-10, IL-12p70, or TNF-α could not be detected either in supernatants of control cells or in cell culture media of HUVECs treated with either one of the 2 Stxs (data not shown). GM-CSF

expression of HUVECs was elevated only after treatment with Stx2, leading to a slight raise after 4 hours and a 4-fold increase after 24 hours, compared with control cells (Figure 7). Furthermore, both Stxs induced higher expression levels of GRO-1 and MCP-1 protein in cell culture supernatants after 24 hours, with Stx2 having a greater impact than Stx1, as shown in Figure 8A-B.

Discussion

Enterohemorrhagic *E coli*, a highly contagious pathogen that has the capacity to cause individual cases of severe illness as well as large outbreaks, carries several pathogenicity factors, among which a family of potent cytotoxins called Stx1 and Stx2 are of key importance.³ Vascular lesions, described as thrombotic microangiopathy, are the morphologic hallmark of HUS,⁷ the most severe clinical manifestation of EHEC disease. For many years, it was assumed that the only relevant biologic activity of Stx was the destruction of cells through inhibition of protein synthesis.^{9,11} However, 4 years ago Bitzan et al reported that Stxs potently increased select mRNA transcript levels in endothelial cells at concentrations that had minimal effects on protein synthesis.¹³ Based on these observations, we incubated human endothelial cells

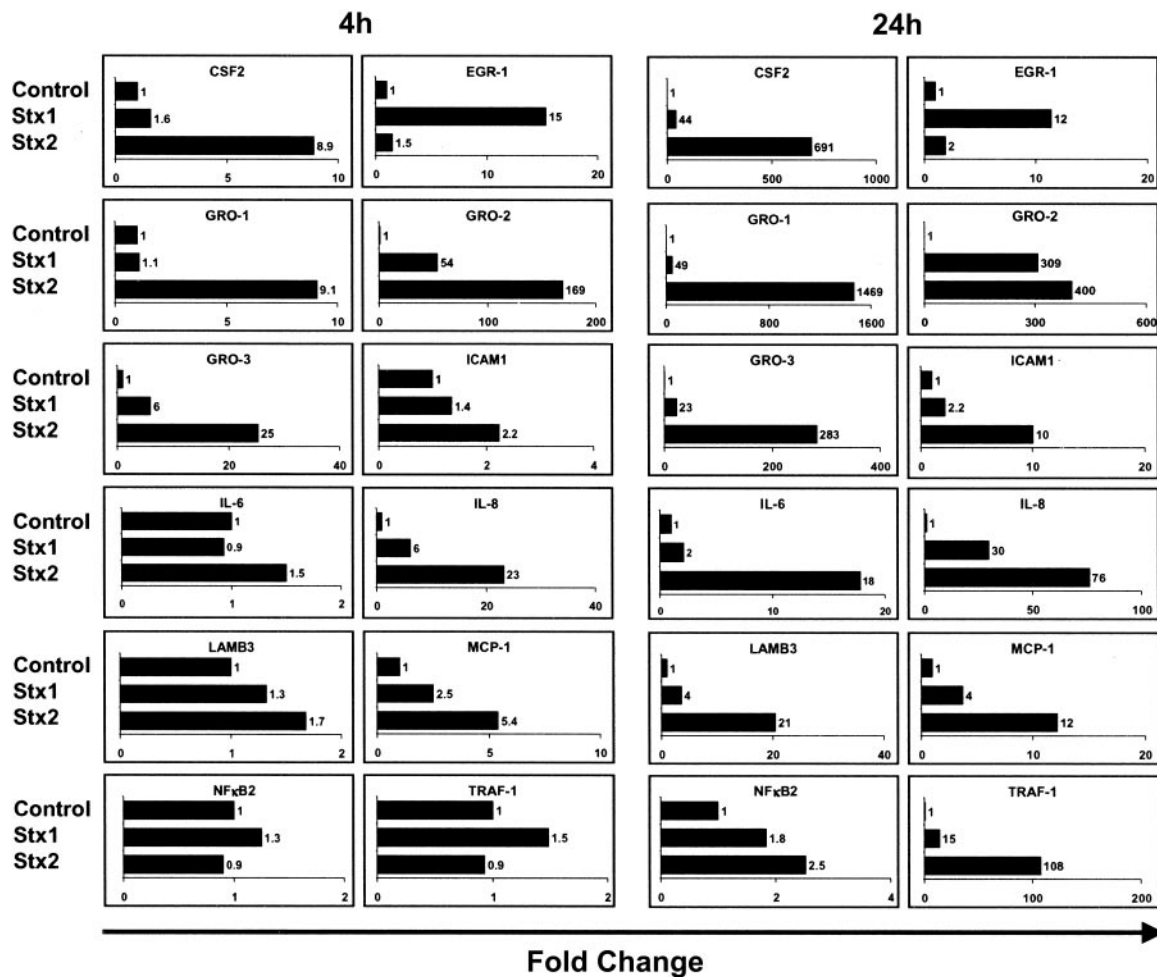


Figure 4. Quantification of gene expression by real-time RT-PCR. Quantitative real-time RT-PCR of 12 genes was performed after 4 hours and 24 hours of incubation with Stxs. Data shown were obtained from 2 independent experiments. CSF2 indicates colony-stimulating factor 2 (granulocyte-macrophage); EGR-1, early growth response 1; GRO-1, GRO-1 oncogene; GRO-2, GRO-2 oncogene; GRO-3, GRO-3 oncogene; ICAM1, intercellular adhesion molecule-1; IL-6, interleukin 6; IL-8, interleukin 8; LAMB3, laminin beta 3; MCP-1, monocyte chemoattractant protein 1; NFκB2, nuclear factor of kappa light polypeptide gene enhancer in B cells 2; and TRAF-1, TNF receptor-associated factor 1.

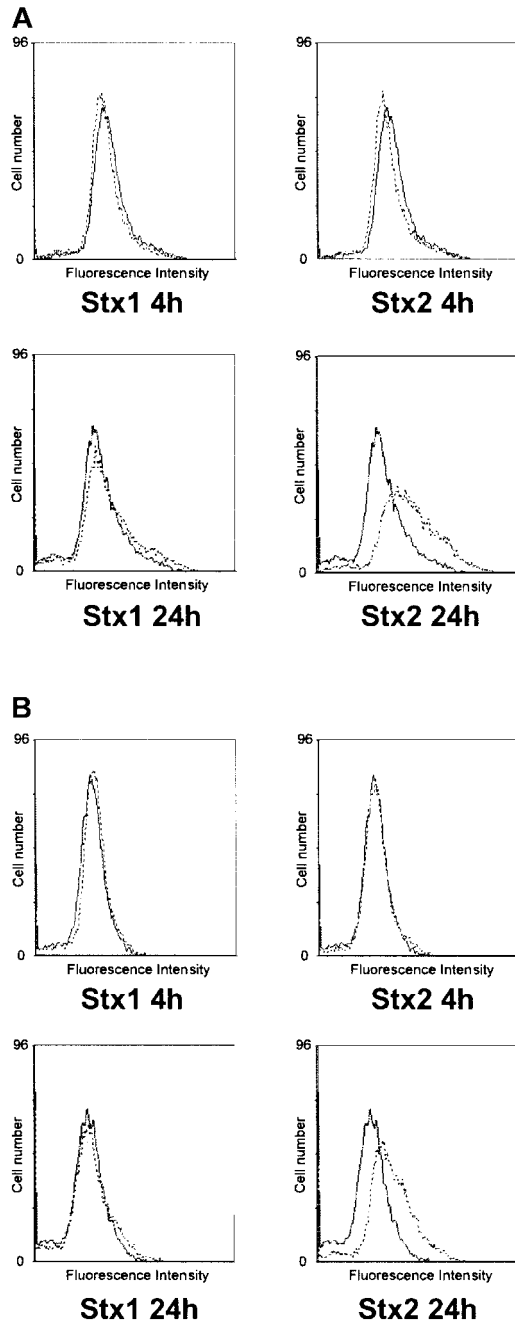


Figure 5. Flow cytometric analysis of CD54 and CD62P expression on HUVECs. In panel A, surface expression of CD54 (intercellular adhesion molecule-1) upon treatment with Stx1 or Stx2 for 4 hours and 24 hours is illustrated (dashed lines) in comparison with untreated control cells (solid lines). The same layout is used in panel B for presentation of flow cytometric data obtained with a CD62P (P-selectin)-specific antibody. The data shown represent 3 independent experiments.

with 1/10 LD₅₀ of Stx1 and Stx2 to investigate genome-wide response patterns using gene expression analysis arrays. Furthermore, such subinhibitory toxin concentrations are also very likely to correspond to the situation in human EHEC disease, since concentrations of Stxs in patient sera are expected to be low²⁵ and antibodies against these proteins are not consistently produced.^{26,27} To verify a regulatory effect of the chosen toxin concentration, we performed RT-PCR with primers specific for the human IL-8 gene, prior to array analysis. HUVECs exhibited a strong regulation of this gene, comparable with data reported by Thorpe et al for intestinal epithelial cells.²⁸

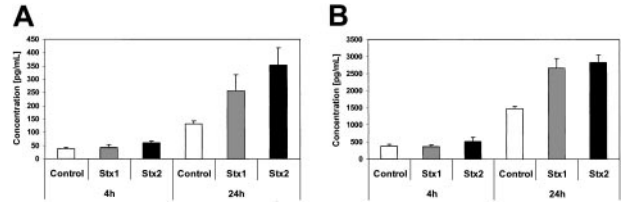


Figure 6. Quantification of IL-6 and IL-8 secretion by CBA analysis. Interleukin-6 (A) and interleukin-8 (B) concentrations in tissue culture supernatants of control cells and HUVECs incubated with Stx1 or Stx2 for 4 hours and 24 hours, measured by cytometric bead array. Data are presented as mean from 3 independent experiments.

Another goal of our study was to decipher potential differences between the mode of action of Stx1 and Stx2 that might explain the high incidence of Stx2 producing *E coli* in patients with severe disease. Much to our surprise, only 25 genes were regulated altogether upon Stx1 incubation and 24 genes by Stx2, despite the fact that we had used arrays representing 6800 and 12 488 human genes, respectively. Most of the regulated genes belonged to chemokines and cytokines. Other ones encoded for cell adhesion molecules and transcription factors that are involved in immune responses or apoptosis, and some genes could not be assigned to a special gene family.

Cytokines are crucial in regulating a variety of molecular and cellular events in inflammation.¹² Genes encoding for IL-8 and GRO-1, -2, and -3 were up-regulated in HUVECs by both Stxs. Thorpe et al had reported similar data for intestinal epithelial cells.¹⁰ Additionally IL-6 and MCP-1 mRNA levels were more abundant upon Stx2 stimulation, although at protein level both toxins led to an increased expression. IL-8 is a C-X-C chemokine that is expressed by various cell types and is strongly up-regulated in endothelial cells by proinflammatory cytokines²⁹ or histamine.³⁰ It increases the binding strength of leukocytes to endothelial cells, thus facilitating their infiltration into an area of inflammation.³¹ Elevated IL-6 and IL-8 levels are found in serum and urine of HUS patients.³ MCP-1 belongs to the family of C-C chemokines,¹² and gene regulation of MCP-1 was observed by array analysis only in HUVECs stimulated with Stx2. Recently, Zoja et al reported an increased expression of MCP-1 mRNA in HUVECs exposed to Stx2.³² Surprisingly, real time RT-PCR revealed regulation also in human endothelial cells incubated with Stx1. RT-PCR data were confirmed by testing of tissue culture supernatants for MCP-1 protein expression using an enzyme immunoassay. This lack of *MCP-1* regulation might be due to a lower sensitivity of array analysis compared with real-time RT-PCR.

GM-CSF is a colony-stimulating factor that stimulates the maturation and differentiation of hematopoietic progenitor cells into granulocytes, macrophages, and erythrocytes, and plays a critical role in the host defense response during infection. GM-CSF is encoded by the *CSF2* gene.³³ Both Stxs had positive effects on

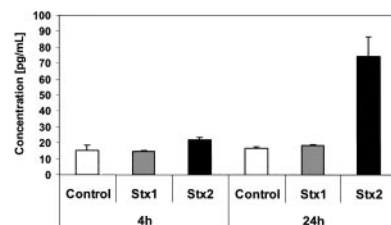


Figure 7. Quantification of GM-CSF secretion by ELISA. GM-CSF levels in tissue culture supernatants from endothelial cells with and without Stx treatment for 4 hours and 24 hours were quantified by ELISA. Data are presented as mean from 3 independent experiments.

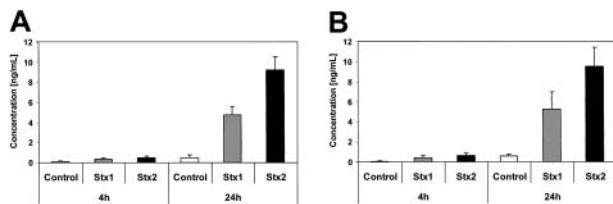


Figure 8. Quantification of GRO-1 and MCP-1 secretion by ELISA. Concentration of GRO-1 oncogene (A) and MCP-1 chemotactic factor (B) are measured by ELISA in culture supernatants of controls and human endothelial cells treated with Stx1 or Stx2 holotoxin for 4 hours and 24 hours. Data are presented as mean from 3 independent experiments.

CSF2 gene regulation, but Stx2 acted faster and more efficiently both on mRNA and protein level and was most prominent after 24 hours. In our experimental setup, Stxs did not induce secretion of IL-1 β and TNF- α . Similar observations had been reported by Sakiri et al³⁴ for human vascular endothelial cells. The proinflammatory effects of certain cytokines seem to play an important role in the development of EHEC disease and may have a major influence on the outcome of HUS.³

The entry of leukocytes into sites of injury or infection requires molecular mechanisms that enable the cells to recognize and form contact points with the endothelium in order to migrate through the blood vessel wall. The extravasation of leukocytes is a multistep process. Selectins on the vessels capture flowing leukocytes and ICAM1 and VCAM1 firmly attach them to the endothelial cells (ECs). Attachment is then followed by extravasation between EC junctions.¹² In the present study we show that only Stx2 induced expression of membrane bound P-Selectin and ICAM1 on HUVECs at subinhibitory concentrations. P-Selectin was expressed at the cell surface with no regulation measurable by array analysis, indicating that this molecule might rather be regulated on translational level. Impact of Stx2 on regulation and expression of cytokine genes and cell adhesion molecules was greater than that of Stx1, delivering potential insights into the epidemiologically well-established fact that systemic complications are more often associated with infections caused by Stx2 producing EHEC strains than with Stx1 producers.³⁵

Furthermore, a number of transcription factors was regulated in HUVECs upon stimulation with Stxs. The transcription factors in most cases belonged to the TNF/stress-related signaling pathway (TRAF-1, TNF α IP-2 and -3) and NF κ B (I κ α , I κ ϵ , N κ B2, FOS,

JUNB, and RelB) pathway. These transcription factors play important roles in immune regulation, cell proliferation, regulation of proinflammatory cytokines, and apoptosis.³⁶ The early growth response (*EGR-1*) gene product is a zinc finger protein transcription factor involved in regulating genes differentially expressed in vascular lesions. It also plays a crucial role in proliferation and activation of smooth muscle cells in the case of endothelial cell damage.³⁷ Increased *EGR-1* expression induces transcription of NAB2 (*EGR-1* binding protein 2), which plays a major role in hemostasis.³⁸ In our experiments only Stx1 induced *EGR-1* gene expression in HUVECs. The lack of *EGR-1* expression of human endothelial cells after exposure to Stx2 may lead to dysfunctions in hemostasis and inadequate responses to the endothelial damage caused by this toxin, ultimately resulting in the occlusion of small vessels. The transcription factor NF κ B is involved in expression of cytokines and cell adhesion molecules in endothelial cells, and is important for the cellular response to damage or infection of the endothelium.³⁹ In the present study we found regulation of I κ α , I κ ϵ , N κ B2, and RelB, though no consistent pattern was observed. These transcription factors are directly involved in the regulation of NF κ B,³⁶ which further emphasizes the proinflammatory effects of Stxs. In addition, both TRAF-1 and TNF α IP-3 were induced after incubation with Stx1 and Stx2 after 24 hours. These transcription factors are important in controlling apoptosis.⁴⁰

From our data, it can be concluded that subinhibitory concentrations of Stxs mediate inflammatory responses of human endothelial cells, which might well be the starting point for the endothelial damage seen in HUS. In addition, among many similarities we were able to identify clear differences in gene regulation and expression between Stx1 and Stx2, regarding cell adhesion molecules and proteins involved in hematopoiesis, hemostasis, and endothelial repair, which could give an explanation for the varying virulence of the 2 toxins in human EHEC disease.

Acknowledgments

We would like to thank Oliver Fuerst and Tanja Toepfer for excellent technical support and Lars Macke for CBA analysis of IL-6 and IL-8. The authors also gratefully acknowledge Klaus Ebnet for helpful discussions and Christofer Samuelsson for assistance in preparing the manuscript.

References

- Paton AW, Ratcliff RM, Doyle RM, et al. Molecular microbiological investigation of an outbreak of hemolytic-uremic syndrome caused by dry fermented sausage contaminated with Shiga-like toxin-producing *Escherichia coli*. *J Clin Microbiol*. 1996;34:1622-1627.
- Paton JC, Paton AW. Pathogenesis and diagnosis of Shiga toxin-producing *Escherichia coli* infections. *Clin Microbiol Rev*. 1998;11:450-479.
- Proulx F, Seidman EG, Karpman D. Pathogenesis of Shiga toxin-associated hemolytic uremic syndrome. *Pediatr Res*. 2001;50:163-171.
- Boerlin P, McEwen SA, Boerlin-Petzold F, et al. Associations between virulence factors of Shiga toxin-producing *Escherichia coli* and disease in humans. *J Clin Microbiol*. 1999;37:497-503.
- Scotland SM, Willshaw GA, Smith HR, Rowe B. Properties of strains of *Escherichia coli* belonging to serogroup O157 with special reference to production of Vero cytotoxins VT1 and VT2. *Epidemiol Infect*. 1987;99:613-624.
- Thomas A, Chart H, Cheasty T, et al. Vero cytotoxin-producing *Escherichia coli*, particularly serogroup O 157, associated with human infections in the United Kingdom: 1989-91. *Epidemiol Infect*. 1993;110:591-600.
- Laszik Z, Silva FG. Hemolytic uremic syndrome, thrombotic thrombocytopenic purpura, and systemic sclerosis (systemic scleroderma). In: Jennette JC, Olson JL, Schwartz MM, Silva FG, eds. *Heptinstall's Pathology of the Kidney*. Philadelphia, PA: Lippincott-Raven Publishers; 1998: 1003-1057.
- Acheson DW, Moore R, De Breucker S, et al. Translocation of Shiga toxin across polarized intestinal cells in tissue culture. *Infect Immun*. 1996;64:3294-3300.
- Endo Y, Tsurugi K, Yutsudo T, et al. Site of action of a Vero toxin (VT2) from *Escherichia coli* O157:H7 and of Shiga toxin on eukaryotic ribosomes: RNA N-glycosidase activity of the toxins. *Eur J Biochem*. 1988;171:45-50.
- Thorpe CM, Smith WE, Hurley BP, Acheson DW. Shiga toxins induce, superinduce, and stabilize a variety of C-X-C chemokine mRNAs in intestinal epithelial cells, resulting in increased chemokine expression. *Infect Immun*. 2001;69:6140-6147.
- Morigi M, Galbusera M, Binda E, et al. Verotoxin-1-induced up-regulation of adhesive molecules renders microvascular endothelial cells thrombogenic at high shear stress. *Blood*. 2001;98:1828-1835.
- Ebnet K, Vestweber D. Molecular mechanisms that control leukocyte extravasation: the selectins and the chemokines. *Histochem Cell Biol*. 1999; 112:1-23.
- Bitzan MM, Wang Y, Lin J, Marsden PA. Verotoxin and ricin have novel effects on preendothelin-1 expression but fail to modify nitric oxide synthase (eNOS) expression and NO production in vascular endothelium. *J Clin Invest*. 1998;101: 372-382.
- Chen R, Lowe L, Wilson JD, et al. Simultaneous quantification of six human cytokines in a single sample using microparticle-based flow cytometric technology. *Clin Chem*. 1999;45:1693-1694.
- Donohue-Rofe A, Acheson DW, Kane AV,

- Keusch GT. Purification of Shiga toxin and Shiga-like toxins I and II by receptor analog affinity chromatography with immobilized P1 glycoprotein and production of cross-reactive monoclonal antibodies. *Infect Immun*. 1989;57:3888-3893.
16. Griffin PM, Ostroff SM, Tauxe RV, et al. Illnesses associated with *Escherichia coli* O157:H7 infections: a broad clinical spectrum. *Ann Intern Med*. 1988;109:705-712.
 17. Liddell KG. *Escherichia coli* O157: outbreak in central Scotland [letter]. *Lancet*. 1997;349:502-503.
 18. Gunzer F, Bohn U, Fuchs S, et al. Construction and characterization of an isogenic *slt-ii* deletion mutant of enterohemorrhagic *Escherichia coli*. *Infect Immun*. 1998;66:2337-2341.
 19. Laemmli UK. Cleavage of structural proteins during the assembly of the head of bacteriophage T4. *Nature*. 1970;227:680-685.
 20. Merrill CR, Switzer RC, Van Keuren ML. Trace polypeptides in cellular extracts and human body fluids detected by two-dimensional electrophoresis and a highly sensitive silver stain. *Proc Natl Acad Sci U S A*. 1979;76:4335-4339.
 21. Switzer RC III, Merrill CR, Shifrin S. A highly sensitive silver stain for detecting proteins and peptides in polyacrylamide gels. *Anal Biochem*. 1979;98:231-237.
 22. Spurr AR. A low-viscosity epoxy resin embedding medium for electron microscopy. *J Ultrastruct Res*. 1969;26:31-43.
 23. Lockhart DJ, Dong H, Byrne MC, et al. Expression monitoring by hybridization to high-density oligonucleotide arrays. *Nat Biotechnol*. 1996;14:1675-1680.
 24. Schrader AJ, Lechner O, Templin M, et al. CXCR4/CXCL12 expression and signalling in kidney cancer. *Br J Cancer*. 2002;86:1250-1256.
 25. Chart H, Law D, Rowe B, Acheson DW. Patients with haemolytic uraemic syndrome caused by *Escherichia coli* O157: absence of antibodies to Vero cytotoxin 1 (VT1) or VT2. *J Clin Pathol*. 1993;46:1053-1054.
 26. Ludwig K, Karmali MA, Sarkim V, et al. Antibody response to Shiga toxins Stx2 and Stx1 in children with enteropathic hemolytic-uremic syndrome. *J Clin Microbiol*. 2001;39:2272-2279.
 27. Ludwig K, Sarkim V, Bitzan M, et al. Shiga toxin-producing *Escherichia coli* infection and antibodies against Stx2 and Stx1 in household contacts of children with enteropathic hemolytic-uremic syndrome. *J Clin Microbiol*. 2002;40:1773-1782.
 28. Thorpe CM, Hurley BP, Lincicome LL, et al. Shiga toxins stimulate secretion of interleukin-8 from intestinal epithelial cells. *Infect Immun*. 1999;67:5985-5993.
 29. Ebnet K, Brown KD, Siebenlist UK, Simon MM, Shaw S. *Borrelia burgdorferi* activates nuclear factor-kappa B and is a potent inducer of chemokine and adhesion molecule gene expression in endothelial cells and fibroblasts. *J Immunol*. 1997;158:3285-3292.
 30. Jeannin P, Delneste Y, Gosset P, et al. Histamine induces interleukin-8 secretion by endothelial cells. *Blood*. 1994;84:2229-2233.
 31. Tangemann K, Gunn MD, Giblin P, Rosen SD. A high endothelial cell-derived chemokine induces rapid, efficient, and subset-selective arrest of rolling T lymphocytes on a reconstituted endothelial substrate. *J Immunol*. 1998;161:6330-6337.
 32. Zoja C, Angioletti S, Donadelli R, et al. Shiga toxin-2 triggers endothelial leukocyte adhesion and transmigration via NF-kappa B dependent up-regulation of IL-8 and MCP-1. *Kidney Int*. 2002;62:846-856.
 33. Frolova EI, Dolganov GM, Mazo IA, et al. Linkage mapping of the human CSF2 and IL3 genes. *Proc Natl Acad Sci U S A*. 1991;88:4821-4824.
 34. Sakiri R, Ramegowda B, Tesh VL. Shiga toxin type 1 activates tumor necrosis factor-alpha gene transcription and nuclear translocation of the transcriptional activators nuclear factor-kappaB and activator protein-1. *Blood*. 1998;92:558-566.
 35. Donohue-Rolfe A, Kondova I, Oswald S, Hutto D, Tzipori S. *Escherichia coli* O157: H7 strains that express Shiga toxin (Stx) 2 alone are more neurotropic for gnotobiotic piglets than are isotypes producing only Stx1 or both Stx1 and Stx2. *J Infect Dis*. 2000;181:1825-1829.
 36. Ghosh S, May MJ, Kopp EB. NF-kappa B and Rel proteins: evolutionarily conserved mediators of immune responses. *Annu Rev Immunol*. 1998;16:225-260.
 37. Santiago FS, Atkins DG, Khachigian LM. Vascular smooth muscle cell proliferation and regrowth after mechanical injury in vitro are Egr-1/NGFI-A-dependent. *Am J Pathol*. 1999;155:897-905.
 38. Khachigian LM, Collins T. Inducible expression of Egr-1-dependent genes: a paradigm of transcriptional activation in vascular endothelium. *Circ Res*. 1997;81:457-461.
 39. Karin M, Lin A. NF-kappaB at the crossroads of life and death. *Nat Immunol*. 2002;3:221-227.
 40. Aggarwal BB. Tumor necrosis factors receptor associated signalling molecules and their role in activation of apoptosis, JNK and NF-kappaB. *Ann Rheum Dis*. 2000;59(suppl 1):i6-16.